

# X-ray structure and *in silico* molecular docking of a natural phaeosphaeride A derivative for targets associated with kinase cascades

Victoria V. Abzianidze,<sup>\*a</sup> Vladimir V. Kadochnikov,<sup>a</sup> Diana S. Suponina,<sup>a</sup> Nikita V. Skvortsov,<sup>a</sup> Petr P. Beltyukov,<sup>a</sup> Vladimir N. Babakov,<sup>a</sup> Denis V. Krivorotov,<sup>a</sup> Elena M. Barysheva<sup>b</sup> and Alexander V. Garabadzhiu<sup>c</sup>

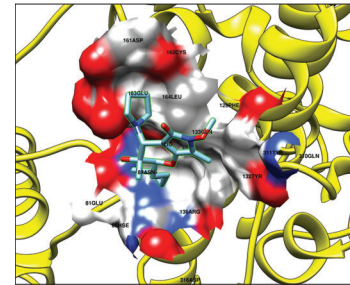
<sup>a</sup> Research Institute of Hygiene, Occupational Pathology and Human Ecology, 188663 Leningrad Region, Russian Federation. E-mail: vyaavy@mail.ru

<sup>b</sup>Research Institute of Carcinogenesis, N. N. Blokhin National Medical Research Center of Oncology, 115478 Moscow, Russian Federation

<sup>c</sup> St. Petersburg State Institute of Technology (Technical University), 190013 St. Petersburg, Russian Federation

DOI: 10.1016/j.mencom.2023.06.030

The structure of the lead compound, a natural phaeosphaeride A derivative AV-6,  $(2S,3R,4R)$ -3-hydroxy-6-methoxy-3-methyl-7-methylene-2-pentyl-4-pyrrolidin-1-yl-3,4,6,7-tetrahydropyrano[2,3-c]pyrrol-5(2H)-one, was unambiguously determined by X-ray crystallography. When modeling *in silico* the interaction of AV-6 with targets in kinase cascades, high values of the binding energy (below  $-9$  kcal mol $^{-1}$ ) for some protein targets were shown. Our results identified that MAPK11, MAPK12 and AKT1 could be targets of AV-6.



**Keywords:** X-ray diffraction analysis, oncology, natural phaeosphaeride A, inhibition of MDR1, *in silico* molecular docking, kinase cascades.

Despite significant progress in the development of drugs for antitumor chemotherapy, there is no universal approach to the creation of a chemotherapeutic agent for the treatment of oncological diseases.<sup>1</sup> Moreover, for some types of tumors, it is not possible to create effective chemotherapy drugs that have the ability to effectively suppress the tumor process by blocking signaling pathways associated with the regulation of proliferative activity, for example, kinase cascades.<sup>2-4</sup> In this regard, the creation of new compounds with potential antitumor activity remains an urgent task. Previously, we synthesized the compounds,<sup>5-7</sup> derivatives of natural phaeosphaeride A,<sup>8</sup> for which cytotoxic effects were demonstrated against a number of tumor cell lines, as well as the ability to inhibit MDR1 (P-gp) and influence the efficiency of phosphorylation in the kinase cascades ERK1/2, JNK and p38 MAPK.<sup>7</sup> **AV-6** turned out to be the only crystalline product of all the leading substances. The main problem was its insolubility in water. Many antitumor compounds are poorly soluble or hydrophobic, which makes it difficult to deliver them to tissues. A large number of research groups are developing new methods of delivering substances to target cells.<sup>9</sup> It seemed important to grow a crystal and determine the crystal structure of **AV-6**. *In silico* determination of possible targets would make it realizable in practice to simplify significantly experiments to determine real targets and, as a result, to select methods for delivering **AV-6** to these targets.

Within the framework of this work, the results of X-ray diffraction analysis of **AV-6** crystals are published for the first time, as well as the results of molecular docking performed using models of potential protein targets involved in intracellular signaling processes and associated with tumor growth. Molecular docking is

an effective tool for analyzing *in silico* the interaction options of new compounds with potential protein targets, from which it is possible to make assumptions about the likely mechanisms of action of potential drugs and to explain the biological effects registered *in vitro* or *in vivo* with cellular or laboratory models.

As part of this approach, X-ray diffraction analysis was made of our lead compound, a natural phaeosphaeride A derivative,<sup>8</sup> **AV-6**<sup>6,7</sup> (Figure 1).<sup>†</sup>

The asymmetric unit of the title compound,  $C_{19}H_{30}N_2O_5$ , contains two independent molecules. **AV-6** contains three primary sections, an alkyl chain consisting of five C atoms, a bicyclic system consisting of five-(envelop-like) and six-(close-

<sup>†</sup> Crystal data for **AV-6**.  $C_{19}H_{30}N_2O_4$  ( $M = 350.45$ ), monoclinic, space group  $P2_1$  at  $100.0(5)$  K,  $a = 11.88260(10)$ ,  $b = 9.55000(10)$  and  $c = 17.21700(10)$  Å,  $\alpha = 90^\circ$ ,  $\beta = 107.8250(10)^\circ$ ,  $\gamma = 90^\circ$ ,  $V = 1859.98(3)$  Å<sup>3</sup>,  $Z = 4$ ,  $d_{\text{calc}} = 1.251$ ,  $\mu(\text{CuK}\alpha) = 0.707$  mm<sup>-1</sup>,  $F(000) = 760.0$ . Measured were 28159 reflections ( $5.392^\circ \leq 2\theta \leq 139.968^\circ$ ), 7060 unique ( $R_{\text{int}} = 0.0345$ ,  $R_{\text{sigma}} = 0.0306$ ) which were used in all calculations. The final  $R1$  was 0.0295 [ $I > 2\sigma(I)$ ] and  $wR2$  was 0.0757 (all data).

X-ray diffraction data were collected on an XtaLAB Synergy, Single source at home/near, HyPix diffractometer. Using Olex2,<sup>10</sup> the structure was solved with the ShelXT<sup>11</sup> structure solution program using intrinsic phasing and refined with the ShelXL<sup>12</sup> refinement package using least squares minimization. XRD analysis was performed at the X-ray Diffraction Centre of St. Petersburg State University (Russian Federation).

CCDC 2244835 contains the supplementary crystallographic data for this paper. These data can be obtained free of charge from The Cambridge Crystallographic Data Centre via <http://www.ccdc.cam.ac.uk>.

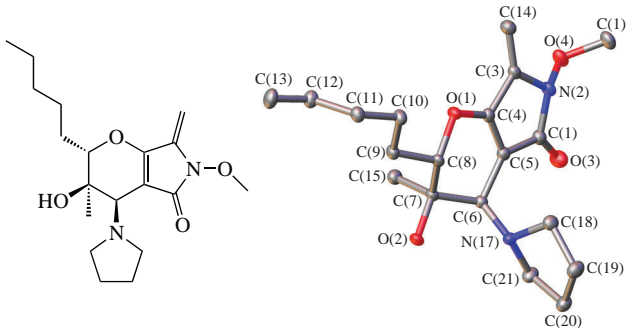


**Figure 1** X-ray crystal structure of AV-6; hydrogens are omitted for clarity.

to planar) membered rings with attached substituents and a pyrrolidine ring adjacent by N(17) to C(6) atom of the bicyclic system, which also exhibits an envelope conformation.

Molecule B is characterized by an intramolecular hydrogen bond between N(17') and a hydrogen atom of the O(2')H hydroxyl group. In the crystal, the molecules form layered structures. Molecules of each type, A or B, form bilayers. In the bilayer, the molecules are arranged antiparallel, and intermolecular hydrogen bonds between oxygen atoms of hydroxyl groups and hydrogen atoms of the pentyl chains participate in the formation of bilayers.

In turn, there are hydrogen bonds between the bilayers, between the oxygen atoms of the methoxy groups and the hydrogens of the exocyclic double bonds of a five-membered cycle of the bicyclic fragment. The pentyl chains of adjacent bilayers are directed towards each other.

The molecular docking was performed for a number of protein targets using the SwissDock service (<http://www.swissdock.ch>).

In addition to the AV-6 molecule, other ligands from the corresponding files in the protein data base (PDB) were used. Some derivatives of natural phaeosphaeride A activate intracellular stress-activated signaling kinase cascades. In an experiment on human epidermoid carcinoma cells A431, we previously showed the induction of phosphorylation and activation of ERK 1/2 (pThr185/pTyr187), JNK (pThr183/pTyr185), and p38 (pThr180/pTyr182).<sup>7</sup>

Proteins involved in the implementation of kinase cascades were considered as potential protein targets for docking, both protein kinases *per se* and their protein targets involved in the regulation of cell growth and differentiation: ERK2/MAPK1, JNK/MAPK8, AKT1, MAPK11, MAPK12, MAPK13, MAPK14, STAT1, STAT3, and STAT5B. Docking was performed for the entire available surface of proteins. Ligands from the pdf format were converted to the mol2 format using a tool available on the website <https://datascience.unm.edu/tomcat/biocomp/convert>.<sup>‡</sup>

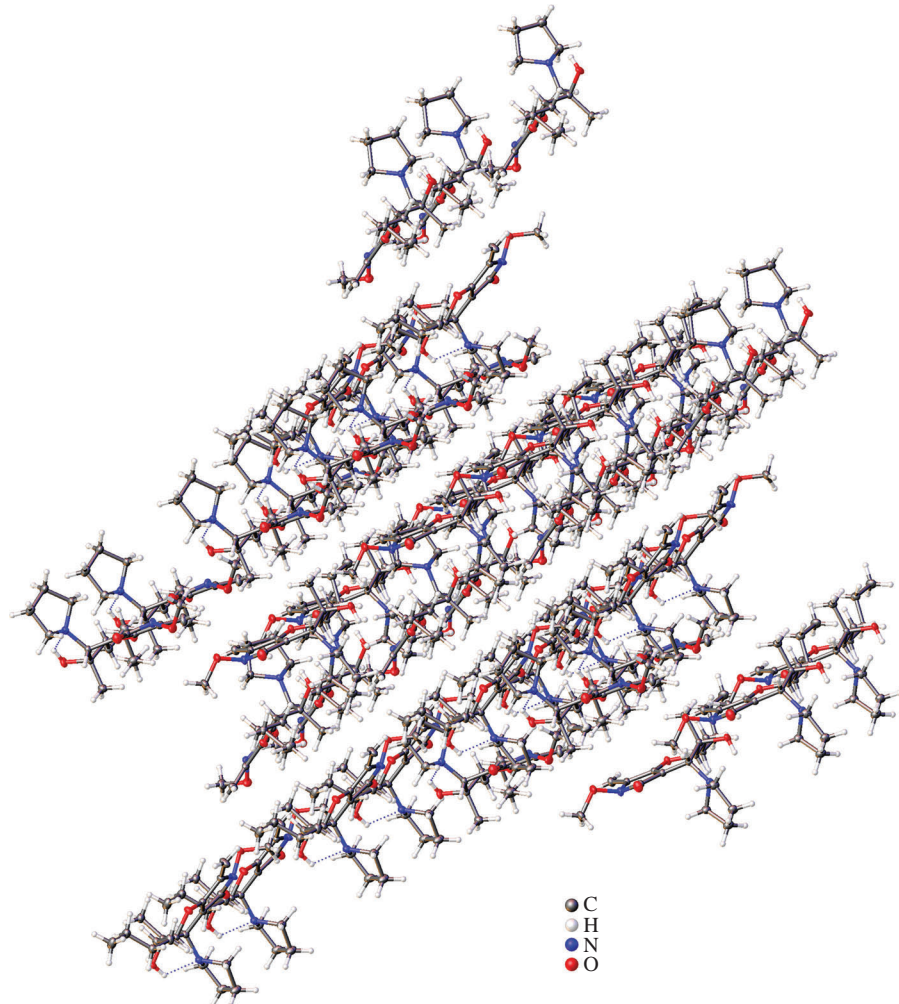


**Figure 2** Bilayers in the AV-6 crystal.

<sup>‡</sup> ERK2 pdb:7w5o; signal transducer and activator of transcription 1-alpha/beta STAT1 pdb:1yvl; signal transducer and activator of transcription 3 STAT3 (APRF); signal transducer and activator of transcription 5B STAT5B; mitogen-activated kinase p38 (pT180/pY182) MAPK11 (PRKM11, SAPK2, SAPK2B) pdb:3gp0; mitogen-activated protein kinase 12

MAPK12 (ERK6, SAPK3) pdb:1cm8; mitogen-activated protein kinase 13 MAPK13 (PRKM13, SAPK4); pdb: 4yn0; mitogen-activated protein kinase 14 MAPK14 (CSBP, CSBP1, CSBP2, CSPB1, MXI2, SAPK2A) pdb:6sfi; stress-activated protein kinase JNK (pT183/pY185) MAPK8 pdb:4qtd; RAC-alpha serine/threonine-protein kinase AKT1 (PKB, RAC) pdb:6hhj.

**Table 1** Calculated binding energy values of **AV-6** and other ligands with kinases.

PDB code	Kinase	$\Delta G/\text{kcal mol}^{-1}$	Ligand
7w5o_chainAB	ERK2	-9.09	6GI
7w5o_chainAB	ERK2	-8.29	5ID
7w5o_chainA	ERK2	-9.66	6GI
7w5o_chainA	ERK2	-8.24	AV-6
7w5o_chainA	ERK2	-7.75	5ID
1yvl	STAT1	-7.62	AV-6
6mwb_chainA	STAT5B	-8.38	AV-6
6mwb_chainB	STAT5B	-8.16	AV-6
6tlc_chainB	STAT3	-8.10	AV-6
6tlc_chainA	STAT3	-8.30	AV-6
4qtb_chainAB	ERK1	-8.15	AV-6
3gp0	MAPK11	<b>-8.96</b>	AV-6
3gp0	MAPK11	-8.30	B45
3gp0	MAPK11	-9.58	Nilotinib
1cm8	MAPK12	<b>-9.01</b>	AV-6
1cm8	MAPK12	-10.32	ANP
4yn0	MAPK13	-7.90	AV-6
4yn0	MAPK13	-8.00	N17
6sf1	MAPK14	-7.53	AV-6
6sf1	MAPK14	-7.51	D13
6sf1	MAPK14	-10.73	LB5
4qtb	MAPK8	-8.25	ANP
4qtb	MAPK8	-8.00	AV-6
6hhj	AKT1	-8.72	AV-6
6hhj	AKT1	-10.99	GH4

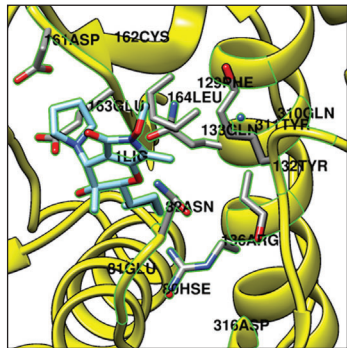
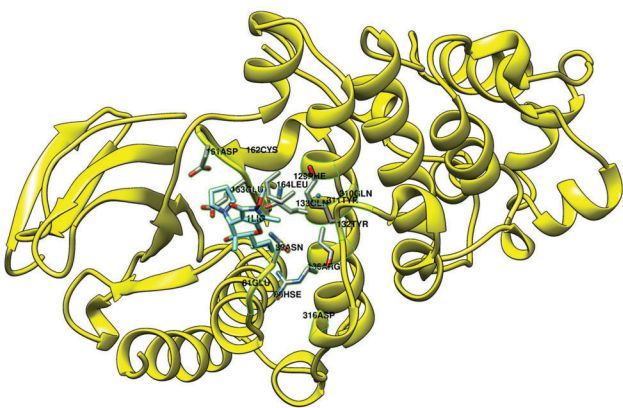


**Figure 3** Binding of AV-6 to MAPK11; marked are amino acid residues, which are located at a distance of 5 Å or less to the ligand.

Information about the protein models used and data on the binding energy estimation of **AV-6** and other ligands with protein targets are presented in Table 1.

When modeling the interaction of **AV-6** with its targets in kinase cascades, high values of the Gibbs free energy change at a level of about 9 kcal mol<sup>-1</sup> for some protein targets were revealed; they are shown in Table 1 (bold-faced).

Based on the results of *in silico* modeling of the interaction of AV-6 with proteins involved in the intracellular kinase cascades, we suggest a probability of direct binding to MAPK11, MAPK12 and AKT1 protein targets. The previously described effects associated with the kinase cascades and identified in *in vitro* cell models, may also be due to the direct effects of AV-6 on these targets. Now it will be easier in practice to fulfill experiments to determine real targets and to select methods for delivering AV-6 to these targets.

## *Online Supplementary Materials*

Supplementary data associated with this article can be found in the online version at doi: 10.1016/j.mencom.2023.06.030.

## References

- 1 A. L. Wilson, M. Plebanski and A. N. Stephens, *Curr. Med. Chem.*, 2018, **25**, 4758.
- 2 A. S. Shaw and E. L. Filbert, *Nat. Rev. Immunol.*, 2009, **9**, 47.
- 3 G. S. Martin, *Cancer Cell*, 2003, **4**, 167.
- 4 J. S. Sebolt-Leopold and R. Herrera, *Nat. Rev. Cancer*, 2004, **4**, 937.
- 5 S. A. Zakharenkova, V. V. Abzianidze, N. I. Moiseeva, D. S. Lukina, L. S. Chisty, D. V. Krivorotov and Yu. G. Trishin, *Mendeleev Commun.*, 2021, **31**, 662.
- 6 V. V. Abzianidze, K. P. Efimova, E. K. Poluektova, Yu. G. Trishin and V. A. Kuznetsov, *Mendeleev Commun.*, 2017, **27**, 490.
- 7 V. Abzianidze, N. Moiseeva, D. Suponina, S. Zakharenkova, N. Rogovskaya, L. Laletina, A. Holder, D. Krivorotov, A. Bogachenkov, A. Garabadzhiu, A. Ukolov and V. Kosorukov, *Pharmaceutics*, 2022, **15**, 395.
- 8 K. N. Maloney, W. Hao, J. Xu, J. Gibbons, J. Hucul, D. Roll, S. F. Brady, F. C. Schroeder and J. Clardy, *Org. Lett.*, 2006, **8**, 4067.
- 9 A. Ellert-Miklaszewska, K. Poleszak and B. Kaminska, *Future Med. Chem.*, 2017, **9**, 199.
- 10 O. V. Dolomanov, L. J. Bourhis, R. J. Gildea, J. A. K. Howard and H. Puschmann, *J. Appl. Crystallogr.*, 2009, **42**, 339.
- 11 G. M. Sheldrick, *Acta Crystallogr.*, 2015, **A71**, 3.
- 12 G. M. Sheldrick, *Acta Crystallogr.*, 2015, **C71**, 3.